Revised Version

SFB/CPP-05-77
DESY 05-235
MS-TP-05-32

$N_f = 2$ Lattice QCD and Chiral Perturbation Theory

L. Scorzato[a*], F. Farchioni[b], P. Hofmann[b], K. Jansen[c], I. Montvay[d], G. Münster[b], M. Papinutto[c†], E. E. Scholz[d‡], A. Shindler[c], N. Ukita[d], C. Urbach[ec§], U. Wenger[c¶], I. Wetzorke[c].

[a] Institut für Physik, Humboldt-Universität zu Berlin, Newtonstr. 15, 12489 Berlin, Germany

[b]Institut für Theoretische Physik, Universität Münster, Wilhelm-Klemm-Str. 9, 48149 Münster, Germany

[c]NIC, Platanenallee 6, 15738 Zeuthen, Germany

[d]DESY, Notkestr. 85, 22607 Hamburg, Germany

[e]Institut für Theoretische Physik, Freie Universität Berlin, Arnimallee 14, D-14195 Berlin, Germany.

By employing a twisted mass term, we compare recent results from lattice calculations of $N_f = 2$ dynamical Wilson fermions with Wilson Chiral Perturbation Theory (WChPT). The final goal is to determine some combinations of Gasser-Leutwyler Low Energy Constants (LECs). A wide set of data with different lattice spacings ($a \sim 0.2 - 0.12$ fm), different gauge actions (Wilson plaquette, DBW2) and different quark masses (down to the lowest pion mass allowed by lattice artifacts and including negative quark masses) provide a strong check of the applicability of WChPT in this regime and the scaling behaviours in the continuum limit.

1. Introduction

It was recently recognized [1,2,3] that an important obstacle for the simulation of Lattice QCD with light dynamical quarks comes from the phase structure of Lattice QCD at small quark masses. Lattice artifacts of $O(a^2)$ may prevent the pion mass from being smaller than a certain minimum value. Such a scenario had been predicted – as an alternative to an Aoki phase scenario – in the context of Chiral Perturbation Theory for the Wilson fermion action (WChPT) [4], and confirmed numerically in [1]. These possibilities are not only a feature of all Wilson-like fermions, but also of staggered fermions [5,6,7]. The most disturbing aspect of this problem is that it may be easily overlooked. In fact very long Monte Carlo histories have been observed, which eventually turned out to be meta-stable points when jumping to a higher value of the pion mass [1]. In the case of pure Wilson fermions long metastable HMC histories ($\sim$ 1000 trajectories) have been recently observed (before converging to a single point) even for lattice spacings as low as $a \approx 0.08$ fm and pion masses $m_\pi \approx 300$ MeV [8]. Even if dangerous, the problem has a simple solution (although for an additional cost): the comparison of simulations at positive and negative quark masses allows to recognize where metastabilities appear.

In this scenario the effect of the gauge action has proved to play an important role. In particular simulations with the DBW2 [9] gauge action showed a considerable decrease of the minimal pion mass [2]. In this work we look in detail into this effect.

The twisted mass fermion approach [10] (tmQCD) provides, among other advantages, the

*Speaker
†Present Address: INFN Sezione di Roma 3, Via della Vasca Navale 84, I-00146 Roma, Italy
‡Present Address: Physics Department, Brookhaven National Laboratory, Upton, NY 11973 USA
§Present Address: Theoretical Physics Division, Dept. of Mathematical Sciences, University of Liverpool, Liverpool L69 3BX, UK
¶Present Address: Institute for Theoretical Physics ETH Zürich CH-8093 Zürich, Switzerland

ideal framework for the investigation of the (zero-temperature) phase diagram of lattice QCD with Wilson fermions, see refs. [11,12,13] for reviews on twisted mass fermions in present and past conferences. On the analytical side WChPT [4,14,15], which has been extended to the twisted mass case [16,17,18,19,20], offers an efficient tool to interpret the lattice data.

Recently we have collected a large statistics of lattice data at large and moderate lattice spacing ($a \sim 0.2 - 0.12$ fm), different gauge actions (Wilson plaquette and DBW2) and different quark masses (down to the lowest pion mass allowed by lattice artifacts and including negative quark masses). In this work we show explicitly the comparison between these lattice data and WChPT. Although for reliable physical predictions definitely smaller lattice spacings are needed, also the lattice spacings that we consider here are useful as a starting point for the extrapolation to a continuum limit. Nevertheless, the results of the present work have to be seen as an exploratory study.

By now a good amount of data has been collected also for the tree-level Symanzik improved gauge action (tlSym) [21], which are very promising, but a detailed ChPT analysis is not yet ready. We will only comment briefly on that at the end.

2. Lattice simulations on $N_f = 2$ QCD

2.1. Fermionic and gauge action

The lattice action for a doublet of degenerate twisted mass Wilson fermions (in the so-called "twisted basis") reads

$$S_q = \sum_x \{(\overline{\chi}_x[\mu_\kappa + i\gamma_5\tau_3 a\mu]\chi_x) + -\frac{1}{2}\sum_{\mu=\pm 1}^{\pm 4}(\overline{\chi}_{x+\hat{\mu}}U_{x\mu}[r+\gamma_\mu]\chi_x)\}\ , \quad (1)$$

with $\mu_\kappa \equiv am_0 + 4r = 1/(2\kappa)$, r the Wilson-parameter, set in our simulations to $r = 1$, am_0 the bare "untwisted" quark mass in lattice units (κ is the conventional hopping parameter) and μ the twisted quark mass; we also define $U_{x,-\mu} = U^\dagger_{x-\hat{\mu},\mu}$ and $\gamma_{-\mu} = -\gamma_\mu$.

The first reason for including μ is that the fermionic determinant is free from exceptional configurations when $\mu \neq 0$ [10], which helps to perform numerical simulations with light quarks. The second reason is a general $O(a)$ improvement [22] and the reduced operator mixing [23,24], when $\mu_\kappa = \mu_{\kappa,\mathrm{crit}}$.

For the gauge sector we consider the one-parameter family of actions including planar rectangular (1×2) Wilson loops ($U^{1\times 2}_{x\mu\nu}$):

$$S_g = \beta \sum_x (c_0 \sum_{\mu<\nu;\,\mu,\nu=1}^{4}\{1 - \frac{1}{3}\,\mathrm{Re}\,U^{1\times 1}_{x\mu\nu}\} + + c_1 \sum_{\mu\neq\nu;\,\mu,\nu=1}^{4}\{1 - \frac{1}{3}\,\mathrm{Re}\,U^{1\times 2}_{x\mu\nu}\})\ , \quad (2)$$

with the normalization condition $c_0 = 1 - 8c_1$. We considered three cases: i.) Wilson plaquette gauge action, $c_1 = 0$, ii.) DBW2 gauge action [9], $c_1 = -1.4088$, iii.) tree-level Symanzik improved gauge action (tlSym) [21], $c_1 = -1/12$.

The reason why such variations have been explored relies on the experience [25] that this may improve the spectrum of the Wilson fermion operator.

2.2. Analysis of the data in tmQCD

In this section we review some formulae which are relevant for the analysis of lattice data produced with tmQCD [2]. In fact tmQCD offers new possibilities for the determinations of the basic QCD parameters and renormalization factors.

The twist angle ω defines the chiral rotation relating twisted mass QCD to ordinary QCD. In the case of the vector and axial currents the rotation reads (considering only charged currents, $a = 1, 2$):

$$\hat{V}^a_{x\mu} = Z_V V^a_{x\mu}\cos\omega + \epsilon_{ab} Z_A A^b_{x\mu}\sin\omega, \quad (3)$$

$$\hat{A}^a_{x\mu} = Z_A A^a_{x\mu}\cos\omega + \epsilon_{ab} Z_V V^b_{x\mu}\sin\omega, \quad (4)$$

where the hatted currents on the l.h.s. denote the chiral currents of QCD (physical currents), while the currents on the r.h.s. are the corresponding bilinears of the quark-field in the twisted (χ-) basis. Note that the renormalization constants of these bilinears, Z_V and Z_A, are involved. For a given choice of the lattice parameters, the twist

angle ω is determined by requiring parity conservation for matrix elements of the physical currents [26,2]. Since unknown renormalization constants are involved, *two* conditions are required, our choice being:

$$\sum_{\vec{x}} \langle \hat{V}^+_{x0}\, P^-_y \rangle \;=\; 0 \;, \tag{5}$$

$$\sum_{\vec{x},i} \langle \hat{A}^+_{xi}\, \hat{V}^-_{yi} \rangle \;=\; 0 \;. \tag{6}$$

The solution of Eqs. (5) and (6) with Eqs. (3) and (4) gives a direct determination of the twist angle ω and of the ratio Z_A/Z_V from lattice data, see [2] for details. In particular at full twist where $\omega = \pi/2$ the condition reads $\sum_{\vec{x}} \langle A^+_{x0}\, P^-_y \rangle = 0$. The full twist situation can be also obtained by requiring the vanishing of the PCAC quark mass in the χ basis. Both definitions are optimal in the sense of [20,19,27].

The knowledge of the twist angle is necessary for the determination of physical quantities like the quark mass and the pion decay constant. The *physical* PCAC quark mass m_q^{PCAC} can be obtained from the Ward identity for the physical axial-vector current. An interesting possibility is to use Eqs. (3, 4) and parity restoration together with the conserved vector current of the χ-fields $\tilde{V}^b_{x\mu}$ for which $Z_V = 1$. This gives

$$am_q^{PCAC} = -i \frac{1}{2\sin\omega} \frac{\langle \nabla^*_\mu \tilde{V}^+_{x\mu} P^-_y \rangle}{\langle P^+_x P^-_y \rangle}. \tag{7}$$

Analogously, for the physical pion decay constant f_π we use

$$af_\pi = (am_\pi)^{-1} \langle 0|\hat{A}^+_0(0)|\pi^+\rangle = -i \frac{\langle 0|\tilde{V}^+_0(0)|\pi^+\rangle}{(am_\pi)\sin\omega}. \tag{8}$$

Notice that with this definition the lattice determination of f_π has automatically the correct normalization [28,29].

Finally, the renormalization constant of the vector current Z_V can be determined on the basis of the non-renormalization property of the conserved current $\tilde{V}_{x\mu}$ [30]. In the case of twisted mass QCD we use

$$Z_V = \frac{\langle 0|\tilde{V}^+_0|\pi^+\rangle}{\langle 0|V^+_0|\pi^+\rangle} \;. \tag{9}$$

We also observe that in a mass independent renormalization scheme, the renormalization factors need to be extrapolated to the chiral limit ($m_q^{PCAC} \to 0$). For this choice of renormalization the parity conserving conditions (5), (6), hold up to lattice artifacts.

In this work we consider the lattice data with parameters summarized in Table 1. The scaling behaviour of the data has already been shown in [31]. Here we concentrate on the comparison with ChPT, which is discussed in the next section.

Table 1
Simulation points.

Action	β	a [fm]	$a\mu$	$L^3 \times T$
DBW2	0.67	0.19	0.01	$12^3 \times 24$
DBW2	0.74	0.12	0.0075	$16^3 \times 32$
plaq	5.1	0.20	0.013	$12^3 \times 24$
plaq	5.2	0.16	0.01	$12^3 \times 24$
plaq	5.3	0.14	0.008	$16^3 \times 32$

3. WChPT versus LQCD

The extension of WChPT to the case of adding a twisted mass term was considered in refs. [32,16, 17,19,18,20]. We denote by L_i the usual Gasser-Leutwyler coefficients[33], while W, $\widetilde{W}$ and W' are some combinations of the new LECs associated to $O(ma)$ and $O(a^2)$ lattice artifacts [14,15,19].

The new LECs depend on the lattice action and also – in general – on the definition of the mass parameter, and of the currents.

If $\kappa_{\rm crit}$ is chosen – for instance – from the van-

ishing of $\cos(\omega)$ and if we define ($\mu_R = \mu/Z_P$):

$$m_{\chi R} = Z_S^{-1}\left(\frac{1}{2a\kappa} - \frac{1}{2a\kappa_{\rm crit}}\right), \quad \rho = 2W_0 a,$$
$$\chi = 2B_0\sqrt{m_{\chi R}^2 + \mu_R^2},$$
$$\cos(\omega) = \frac{m_{\chi R}}{\sqrt{m_{\chi R}^2+\mu_R^2}},$$

then we have for the pion mass and the PCAC quark mass:

$$\begin{aligned} m_{\pi\pm}^2 &= \chi + \frac{1}{32\pi^2 F_0^2}\chi^2 \ln\frac{\chi}{(4\pi F_0)^2} + \\ &+\frac{8}{F_0^2}\{(4L_6+2L_8-2L_4-L_5)\chi^2 + \\ &+2(2W-\widetilde{W})\rho\,\chi\cos(\omega) + \\ &+4W'\rho^2\cos(\omega)^2\}, \qquad (10) \\ m_q^{PCAC} &= \frac{Z_P}{2B_0}[\chi + \frac{16}{F_0^2}(W\chi\rho\cos(\omega) + \\ &+2W'\rho^2\cos(\omega)^2)] \qquad (11) \end{aligned}$$

Similar formulae are available for f_π and g_π [19]. These formulae are valid in the regime where $m_q^{PCAC}/\Lambda_{QCD} \gtrsim a\Lambda_{QCD}$, where most of our simulated points are located. In the case of a first order phase transition scenario (as it appears to be the case), the same formulae hold also for smaller masses (although some terms can be dropped). In the regime of very small masses also NLO calculations have been done, leading to the addition of the $O(a^3)$ terms, [34,35], however we will neglect these corrections here.

We first show a qualitative comparison of our data with the formulae above. Figure 1 (left) displays the pion mass in the case of DBW2 gauge action and a relatively large lattice spacing ($a \sim 0.19$ fm). The data for m_π^2 can be reasonably fitted by straight lines (therefore neglecting NLO ChPT terms and the small twisted mass μ). What cannot be neglected is the presence of a minimal pion mass of roughly ~ 300 MeV. No meta-stabilities have been detected. If we compare with Figure 1 (right) – whose data are produced with plaquette gauge action at an even smaller lattice spacing ($a \sim 0.16$ fm) – the striking difference is the presence of a much higher minimal pion mass. Here many meta-stable points have been detected, which did not tunnel into stable ones. Notice that the comparison is done at the same value of μ, and $a\mu$ is larger for the DBW2 case (the effect of μ is however small, at the present value).

This picture is confirmed by the PCAC quark mass. Eq. (11) shows that lattice artifacts break the linear relation between m_q^{PCAC} and χ (they are simply two definitions of the quark mass). In particular the W term induces a difference in the slope at positive and negative quark masses. The term W', instead, is responsible for a jump at the origin, which prevents $|m_q^{PCAC}|$ from being smaller than some $O(a^2)$ lattice artifact. Both these expected features are visible, but small, in Figure 2 (left): two different slopes and a small jump. Also Figure 2 (right) can be understood in terms of such effects, which however completely upset the continuum picture. The scaling behaviour of these effects is confirmed by the other β values in Table 1.

The observation that the optimal critical mass can be determined by the vanishing of m_χ^{PCAC} suggested [2] to express the pion mass (and in general all pionic quantities) as function of the PCAC quark mass instead of $1/\kappa$. The result for m_π is (now $\chi := 2\frac{B_0}{Z_P}\sqrt{(\cos(\omega)m_q^{PCAC})^2+\mu^2}$, other definitions are as above):

$$\begin{aligned} m_{\pi\pm}^2 &= \chi + \frac{1}{32\pi^2 F_0^2}\chi^2 \ln\frac{\chi}{(4\pi F_0)^2} + \\ &+\frac{8}{F_0^2}\{(4L_6+2L_8-2L_4-L_5)\chi^2 \\ &+2(W-\widetilde{W})\rho\,\chi\cos(\omega)\}, \qquad (12) \end{aligned}$$

In this reparametrization the constant W' disappears, – and so does the $O(a^2)$ term – and the pion mass can apparently go to zero when $m_q^{PCAC} \to 0$. However, one should keep in mind that not all values of m_q^{PCAC} are accessible with stable simulation points. This parametrization allows to include in the ChPT fit also meta-stable points, where both m_π and m_q^{PCAC} are lower than it would be possible in a stable minimum of the effective potential. Since this is an interesting check, we exploit this possibility and we include also meta-stable points (from [3]) in the fit.

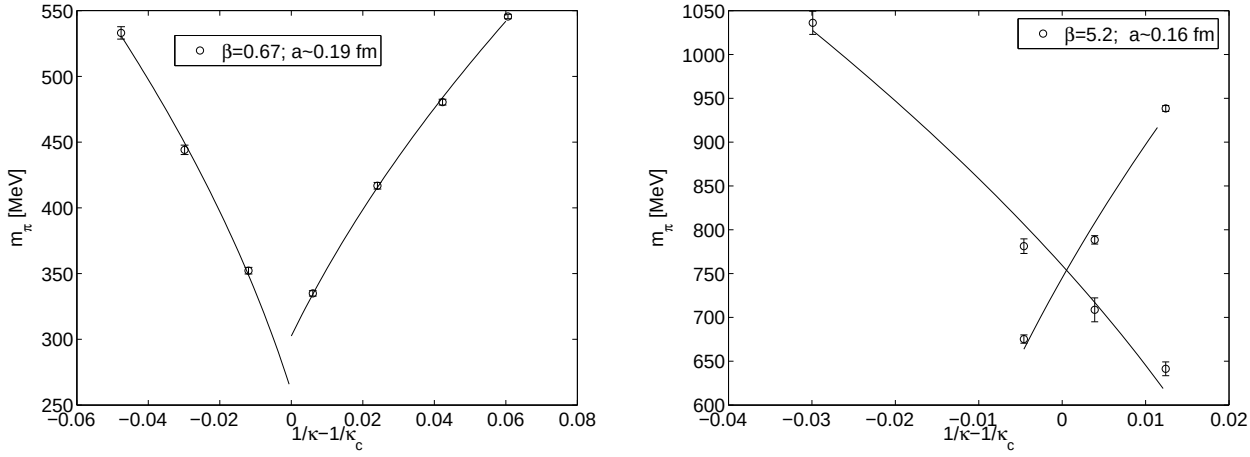

Figure 1. Pion mass for DBW2 (left) and plaquette (right) gauge action at $\beta = 0.67$ (DBW2), and $\beta = 5.2$ (plaquette). For both V= $12^3 \times 24$ and $a\mu = 0.01$. Fit of m_π^2 is done with a linear fit.

Combined fits of m_π, f_π and g_π provide strong constraints. Results for m_π are shown in Figure 3. They give an estimate of $F_0 \simeq 85$ MeV and values for the LECs in agreement with previous estimates [36,37]. Results for the W's appear compatible with zero. Details will be presented elsewhere [38].

4. Conclusions

We have shown a comparison of unquenched lattice data with WChPT. We found that WChPT seems to describe the data rather well and results for low-energy constants are consistent with previous determinations. This lets us be confident that a precise determination will be possible with reasonable computation cost.

WChPT lets us investigate the phase structure of lattice QCD. There is a striking difference on this aspect between DBW2 and plaquette gauge action. It is interesting to vary the coupling c_1 in Eq. (2) and interpolate between DBW2 and plaquette actions. It appears that even a small value of c_1 can already have a large impact on the phase structure. This is illustrated in Figure 4 where we show the average plaquette value as a function of the hopping parameter κ for three different actions, i.e. different values of c_1, namely $c_1 = 0$ (Wilson), $c_1 = -1/12$ (tlSym) and $c_1 = -1.4088$ (DBW2). As one moves κ from the negative or positive side across the critical point,

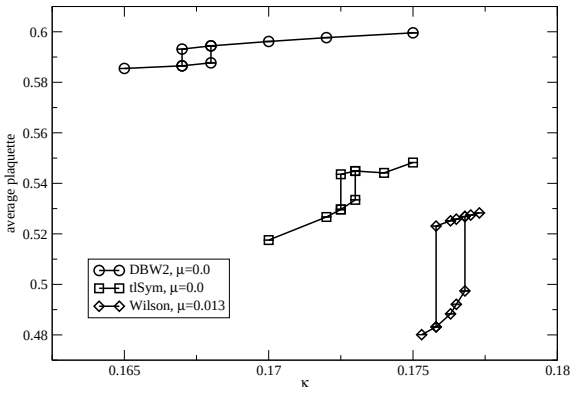

Figure 4. Hysteresis of the average plaquette value as κ is moved across the critical point, for Wilson, tlSym and DBW2 gauge action at $a \sim 0.17$ fm.

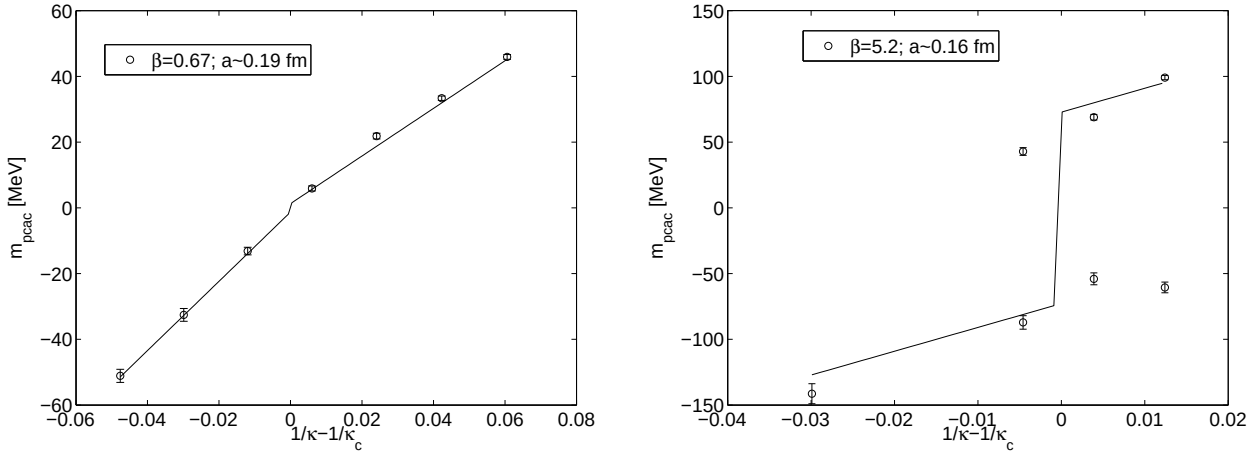

Figure 2. PCAC quark mass for DBW2 (left) and plaquette (right) gauge action at $\beta = 0.67$ (DBW2), and $\beta = 5.2$ (plaquette). For both V= $12^3 \times 24$ and $a\mu = 0.01$. Fits are only qualitative, on the basis of Eq. (11).

where the PCAC quark mass vanishes, a hysteresis in the average plaquette value develops whose size and width are indicators of the strength of the phase transition. We observe that both the width and the size of the gap in the plaquette value decreases considerably as we switch on c_1 to $c_1 = -1/12$ (tlSym action). Decreasing c_1 further down to $c_1 = -1.4088$ (DBW2 action) still seems to reduce the size of the gap, but the effect is surprisingly small despite the large change in c_1. Note that the results in Figure 4 are for a lattice spacing $a \sim 0.17$ fm that is roughly consistent for all three actions. One should remark that the results for the Wilson plaquette gauge action are at non-zero twisted mass $\mu = 0.013$, as opposed to the tlSym and the DBW2 data in the same plot. Since the strength of the phase transition is expected to be reduced as one switches to a non-zero twisted mass, a true comparison at $\mu = 0$ would disfavor the Wilson plaquette gauge action even more.

Comparison of tlSym data with ChPT will be presented elsewhere [39].

Acknowledgments

L.S. wishes to thank the organizers and all the participants of the workshop for the beautiful and stimulating environment. In particular G. Colangelo, M. Golterman, G.C. Rossi and Y. Shamir are acknowledged for very helpful discussions. The computer centers at NIC/DESY Zeuthen, NIC at Forschungszentrum Jülich and HLRN provided the necessary technical help and computer resources. This work was supported by the DFG Sonderforschungsbereich/Transregio SFB/TR9-03.

REFERENCES

1. F. Farchioni *et al.*, Eur. Phys. J. **C39**, 421 (2005), [hep-lat/0406039].
2. F. Farchioni *et al.*, Eur. Phys. J. **C42**, 73 (2005), [hep-lat/0410031].
3. F. Farchioni *et al.*, Phys. Lett. **B624**, 324 (2005), [hep-lat/0506025].
4. S. R. Sharpe and J. Singleton, Robert L., Phys. Rev. **D58**, 074501 (1998), [hep-lat/9804028].
5. W.-J. Lee and S. R. Sharpe, Phys. Rev. **D60**, 114503 (1999), [hep-lat/9905023].
6. C. Aubin and Q.-h. Wang, Phys. Rev. **D70**, 114504 (2004), [hep-lat/0410020].

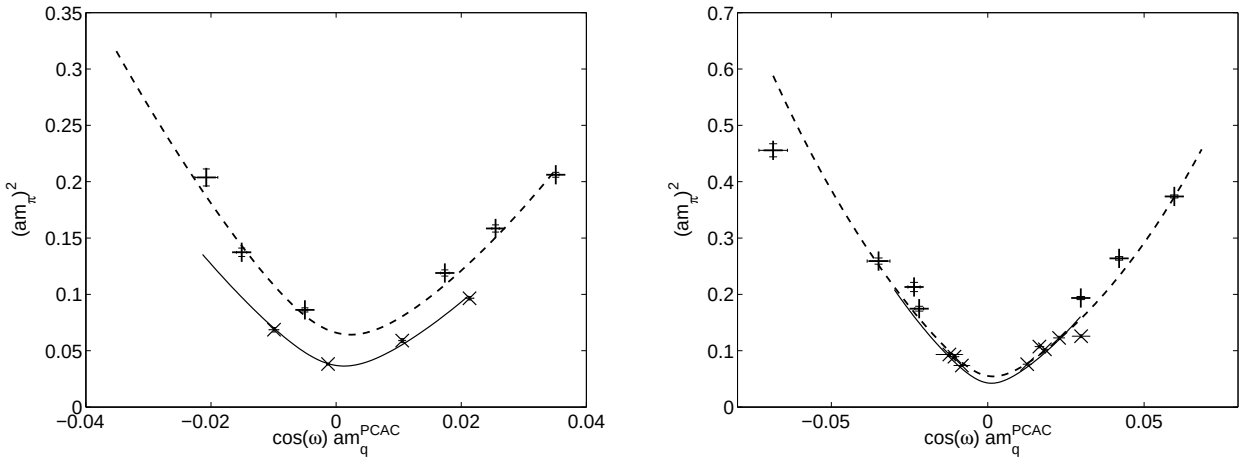

Figure 3. Fit of Eq. (12) against the DBW2 data (left) at $\beta = 0.67$ (dashed line and +) and $\beta = 0.74$ (full line and $\times$) and plaquette data (right) at $\beta = 5.2$ (dashed line and +) and $\beta = 5.3$ (full line and $\times$). Fit are performed in combination with those of f_π and g_π to provide more constraints, although they are not shown.

7. A. Hasenfratz, hep-lat/0511021.
8. K. Jansen, A. Shindler, C. Urbach and U. Wenger, hep-lat/0510064.
9. T. Takaishi, Phys. Rev. **D54**, 1050 (1996).
10. Alpha, R. Frezzotti, P. A. Grassi, S. Sint and P. Weisz, JHEP **08**, 058 (2001), [hep-lat/0101001].
11. R. Frezzotti, Nucl. Phys. Proc. Suppl. **119**, 140 (2003), [hep-lat/0210007].
12. R. Frezzotti, Nucl. Phys. Proc. Suppl. **140**, 134 (2005), [hep-lat/0409138].
13. A. Shindler, hep-lat/0511002.
14. G. Rupak and N. Shoresh, Phys. Rev. **D66**, 054503 (2002), [hep-lat/0201019].
15. O. Bär, G. Rupak and N. Shoresh, Phys. Rev. **D70**, 034508 (2004), [hep-lat/0306021].
16. G. Münster, JHEP **09**, 035 (2004), [hep-lat/0407006].
17. L. Scorzato, Eur. Phys. J. **C37**, 445 (2004), [hep-lat/0407023].
18. S. R. Sharpe and J. M. S. Wu, Phys. Rev. **D70**, 094029 (2004), [hep-lat/0407025].
19. S. R. Sharpe and J. M. S. Wu, Phys. Rev. **D71**, 074501 (2005), [hep-lat/0411021].
20. S. Aoki and O. Bär, Phys. Rev. **D70**, 116011 (2004), [hep-lat/0409006].
21. P. Weisz, Nucl. Phys. **B212**, 1 (1983).
22. R. Frezzotti and G. C. Rossi, JHEP **08**, 007 (2004), [hep-lat/0306014].
23. C. Pena, S. Sint and A. Vladikas, JHEP **09**, 069 (2004), [hep-lat/0405028].
24. R. Frezzotti and G. C. Rossi, JHEP **10**, 070 (2004), [hep-lat/0407002].
25. Y. Aoki *et al.*, Phys. Rev. **D69**, 074504 (2004), [hep-lat/0211023].
26. F. Farchioni *et al.*, Nucl. Phys. Proc. Suppl. **140**, 240 (2005), [hep-lat/0409098].
27. R. Frezzotti, G. Martinelli, M. Papinutto and G. C. Rossi, hep-lat/0503034.
28. R. Frezzotti and S. Sint, Nucl. Phys. Proc. Suppl. **106**, 814 (2002), [hep-lat/0110140].
29. XLF, K. Jansen, A. Shindler, C. Urbach and I. Wetzorke, Phys. Lett. **B586**, 432 (2004), [hep-lat/0312013].
30. L. Maiani and G. Martinelli, Phys. Lett. **B178**, 265 (1986).
31. F. Farchioni *et al.*, hep-lat/0509131.
32. G. Münster and C. Schmidt, Europhys. Lett.

66, 652 (2004), [hep-lat/0311032].
33. J. Gasser and H. Leutwyler, Nucl. Phys. **B250**, 465 (1985).
34. S. R. Sharpe, Phys. Rev. **D72**, 074510 (2005), [hep-lat/0509009].
35. S. Aoki and O. Bär, hep-lat/0509002.
36. qq+q, F. Farchioni, I. Montvay, E. Scholz and L. Scorzato, Eur. Phys. J. **C31**, 227 (2003), [hep-lat/0307002].
37. qq+q, F. Farchioni, I. Montvay and E. Scholz, Eur. Phys. J. **C37**, 197 (2004), [hep-lat/0403014].
38. F. Farchioni *et al.*, in preparation.
39. F. Farchioni *et al.*, in preparation.